JOC The Journal of Organic Chemistry

Note

pubs.acs.org/joc

A Light-Gated Molecular Brake with Antilock and Fluorescence Turn-On Alarm Functions: Application of Singlet-State Adiabatic Cis → Trans Photoisomerization

Wei-Ting Sun, Guan-Jhih Huang, Shou-Ling Huang, Ying-Chih Lin, and Jye-Shane Yang*

Department of Chemistry, National Taiwan University, No 1 Sec 4 Roosevelt Road, Taipei, Taiwan 10617

Supporting Information

ABSTRACT: A light-gated molecular brake that displays both high braking power (~10^7) and high switching power (~74%) is reported. The lower rate for brake-on than for brake-off switching of the pentiptycene rotor mimics the function of an antilock braking system (ABS) for vehicles on a loose surface. The brake is also armed with a fluorescence turn-on alarm for accidental deactivation of the ABS function by acids. All of these features are associated with the highly efficient singlet-state adiabatic cis → trans photoisomerization of the phenylstilbene chromophore.

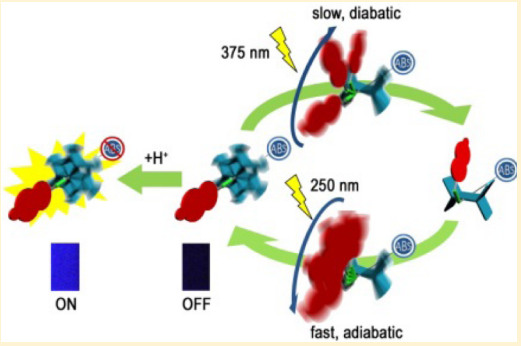

The development of artificial molecular machines continues to be a challenging subject in the field of nanoscience and nanotechnology.[1] Our current ability to control the motions of molecules, particularly the rotary motion about a single bond, is still in the stage of infancy. The concept of "molecular brakes" is aimed to control rotary motions at the molecular level with switchable rotation rates through external stimuli (fuels).[2−6] Among the various forms of fuels, light has the advantages of rapid input, remote control, and no deposition of chemical waste. In addition, the response of molecules to light is not limited to changes in chemical or electronic structures but could also generate photoluminescence signals. However, light-gated molecular brakes with high switching and braking power remained to be demonstrated.

We recently proposed the concept of molecular brakes with an antilock function, namely, a slow braking process but a fast acceleration process, mimicking the function of antilock braking systems (ABSs) for vehicles on loose surfaces.[7] Our first design of a molecular ABS is *t*-**1** (Scheme 1), in which the four-bladed paddlewheel-like pentiptycene is the rotor component, the styryl group is the switchable brake pad, and the amino → stilbene photoinduced electron transfer (PET) is the antilock module.[6] However, it requires the use of chemical fuels (acids and bases) to gate the PET function and thus to reach optimal ABS operation (Scheme 2a), which renders the operation no longer waste-free, remote, and fast. We report herein a new molecular ABS *t*-**2** that is operated without the need of chemical fuels and meanwhile has improved performance in all aspects, including the ABS performance, the braking power, and the switching power. In addition, when the PET is disabled by the presence of acids, strong blue fluorescence is emitted, setting an alarm function for the ABS operation of *t*-**2**.

Scheme 1. Structures and Concept of Light-Gated Molecular ABSs 1 and 2[a]

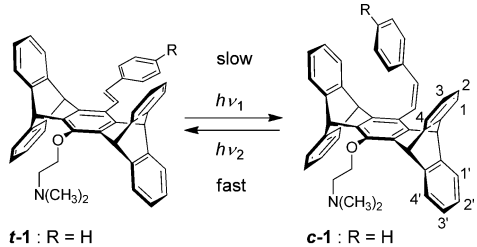

[a]The trans (*t*) and cis (*c*) isomers correspond to the brake-off and brake-on states, respectively. The numeric labels for protons and carbons on the pentiptycene group are for discussion of the NMR spectra.

The synthesis of molecular ABS *t*-**2** was carried out with the Heck coupling between pentiptycene iodide **3** and 4-cyano-4′-vinylbiphenyl (**4**) (Scheme 3). The synthesis of both **3**[6] and **4**[8] have been reported. The cis isomer *c*-**2** was obtained upon irradiation of *t*-**2** in THF at 365 nm.

The rotational kinetics of the pentiptycene rotor in *c*-**2** was investigated by variable-temperature (VT) ^{13}C NMR spectroscopy. The carbon signals on the pentiptycene group can be unambiguously assigned on the basis of a series of 2D NMR experiments, including COSY, HSQC, and NOESY (Figures

Received: March 27, 2014
Published: June 12, 2014

dx.doi.org/10.1021/jo5007015 | J. Org. Chem. 2014, 79, 6321−6325

Scheme 2. Optimal ABS Operation Processes for the Molecular Brakes (a) *t*-1 and (b) *t*-2

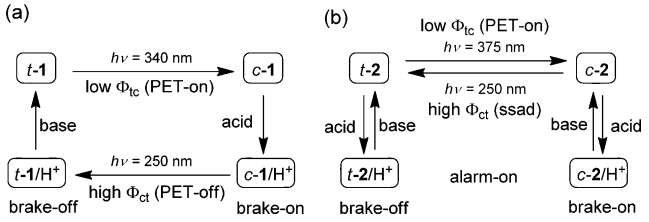

Scheme 3. Synthesis of Molecular ABS *t*-2 and its Isomer *c*-2

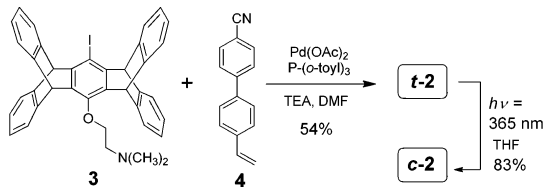

S1–S4 in the Supporting Information). Line shape analysis of the C(1) and C(4) signals and the resulting rate constants for rotation (k) are shown in Figure 1. The activation parameters

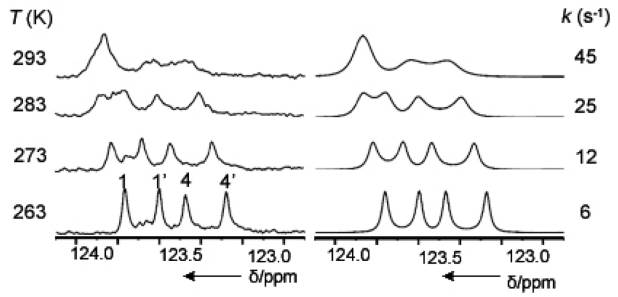

Figure 1. (left) VT ^{13}C NMR (125 MHz) spectra and (right) simulated spectra of *c*-**2** in CD_2Cl_2 at the region of C(1) and C(4) (see Scheme 1 for labels). Values of the temperature (T, K) and rate constant (k, s^{-1}) for interconversion between the two isoenergetic states (i.e., 180° rotation) are also given for each trace.

derived from the Arrhenius and Eyring plots (Figure S5 in the Supporting Information) are listed in Table S1 in the Supporting Information. Compared to *c*-**1**, *c*-**2** displays similar values of the activation barrier (E_a = 10.4 vs 10.6 kcal mol^{-1}) and enthalpy of activation ($\Delta H^{\ddagger}$ = 9.8 vs 10.1 kcal mol^{-1}), but the k value at 293 K is 1 order of magnitude lower (45 vs 670 s^{-1}). As indicated by the smaller preexponential value (log A = 9.4 vs 10.6) and more negative entropy of activation ($\Delta S^{\ddagger}$ = −17.3 vs −11.8 cal mol^{-1} K^{-1}) for *c*-**2** versus *c*-**1**, the elongation of the brake pad mainly causes a larger constraint of the molecule in the rotational transition state. In contrast, the rotation rate for the pentiptycene rotor in *t*-**2** is expected to be the same as that in *t*-**1** (~10^9 s^{-1}), which was evaluated[4] by density functional theory calculations because of the lack of decoalescence of the proton signals even at 183 K (Figure S6 in the Supporting Information). Thus, the braking power is as high as ~10^7 for **2** at ambient temperature and is superior to that of **1** (~10^6).

Figure 2 shows the absorption and fluorescence spectra of *t*-**2** and *c*-**2** in acetonitrile. The absorption maximum (λ_{abs}) is red-shifted by 11 nm for *t*-**2** versus *c*-**2** (Table 1), which could be understood by the more planar π backbone and thus the longer

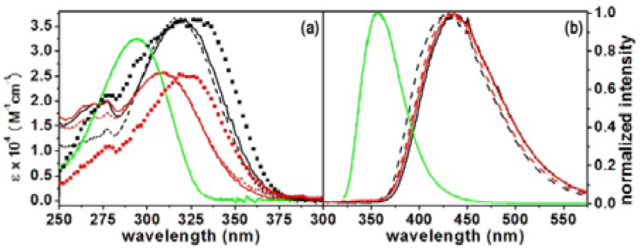

Figure 2. Electronic (a) absorption and (b) emission spectra of *t*-**2** (black), *c*-**2** (red), and **4** (green) in the absence (solid lines) and presence (dashed lines) of 10 equiv of $HClO_4$ in acetonitrile at room temperature. The excitation spectra of *t*-**2** (squares) and *c*-**2** (circles) are also shown in (a) for comparison.

Table 1. Photophysical and Photochemical Data for 1, 2, and 4 in Acetonitrile with and without $HClO_4$[a]

compd	λ_{abs} (nm)	λ_{fl} (nm)	Φ_{fl} (%)	$\Phi_{tc/ct}$ (%)
t-**1** (*t*-**1**/H^+)	267 (267)	–[b]	–[b]	11 (49)
c-**1** (*c*-**1**/H^+)	250 (250)	–[b]	–[b]	20 (45)
t-**2** (*t*-**2**/H^+)	320 (318)	436 (431)	8 (46)	13 (25)
c-**2** (*c*-**2**/H^+)	309 (309)	435 (431)	4 (35)	68 (64)
4 (**4**/H^+)	294 (294)	357 (357)	90 (84)	–[c]

[a]Data in parentheses correspond to the presence of $HClO_4$. [b]The fluorescence was too weak for this to be determined. [c]No cis–trans isomers.

effective conjugation length. However, the fluorescence spectra are essentially the same for the two isomers. In the presence of a strong acid such as $HClO_4$, the long-wavelength absorption bands and the fluorescence spectra of both isomers are unchanged but the fluorescence quantum yields (Φ_{fl}) are increased 6–9-fold. These observations indicate that the amino → phenylstilbene PET has occurred in *t*-**2** and *c*-**2** but is inhibited in *t*-**2**/H^+ and *c*-**2**/H^+, in which the amino group is protonated. In addition, the excitation and emission of the phenylstilbene chromophore do not involve the amino group (i.e., there is no exciplex formation). The ability of *t*-**2** and *c*-**2** to fluoresce is in sharp contrast to the nonfluorescent behavior of *t*-**1** and *c*-**1** and their analogues.[4−6]

Several pieces of information indicate that the fluorescence of *t*-**2** and *c*-**2** results from *t*-**2***, the common excited state of *t*-**2**, indicating that the singlet-state adiabatic (ssad) *c*-**2*** → *t*-**2*** isomerization has occurred. First, the broad emission band with a large Stokes shift (>8000 cm^{-1}) indicates charge-transfer character for the excited states, which is consistent with the dipolar phenylstilbene π system in *t*-**2**. Second, the possibility that the excited state is localized in a π segment such as the 4-cyano-4′-vinylbiphenyl (CVB) moiety can be excluded. Compound **4** corresponds to the CVB moiety in **2**, but its absorption and fluorescence spectra are largely blue-shifted from those of *t*-**2** and *c*-**2**. Evidently, the fluorophore is larger than the CVB moiety and should be the phenylstilbene π system. Third, the excitation spectrum of *t*-**2** differs from that of *c*-**2** (Figure 2a and Figure S7 in the Supporting Information), showing the difference of the excited precursors (*t*-**2*** and *c*-**2***) for the observed fluorescence. The small red shifts of the excitation spectra relative to the corresponding absorption spectra (7–14 nm) indicate a larger Φ_{fl} for the more planar conformers. Fourth, the fluorescence spectra are no longer the same for *t*-**2** and *c*-**2** below 160 K (Figure S8 in the Supporting Information), consistent with the scenario of a slow *c*-**2*** → *t*-

dx.doi.org/10.1021/jo5007015 | J. Org. Chem. 2014, 79, 6321–6325

2* photoisomerization process at low temperatures because of the presence of a torsional barrier. Finally, the cis → trans photoisomerization quantum yield (Φ_{ct}) observed for *c*-**2** is unusually large (0.68) even in the presence of a PET deactivation channel, which could hardly be explained by the conventional diabatic mechanism (vide infra). To date, reports of efficient ssad photoisomerization are limited, and it has been observed only for π-extended stilbene derivatives such as styrylpyrene and distyrylbenzene.[9,10] Our results show that phenylstilbenes (or styrylbiphenyls) are new candidates for ssad cis → trans photoisomerization.

Because of the PET, a low trans → cis isomerization quantum yield (Φ_{tc}) is observed for *t*-**2**, as expected. According to the diabatic one-bond-flip mechanism for stilbenes (Scheme 4, where the *p** → *t** process is negligible),[11] the trans → cis and cis → trans isomerizations adopt the same intermediate, a perpendicularly twisted excited state (*p**), which it undergoes ultrafast internal conversion to the ground state (*p*) followed by partitioning to the trans and cis isomers with similar probabilities (i.e., 50%). This corresponds to a maximum value of ∼0.50 predicted for the quantum yields Φ_{ct} and Φ_{tc}. When fluorescence and other reactions such as the PET in *t*-**2** compete with the decay of the excited state, the relationship $\Phi_{fl}+ \Phi_{PET} + 2\Phi_{tc}$ (or $2\Phi_{ct}$) ≈ 1.0 is expected. Indeed, the relationship $\Phi_{fl} + 2\Phi_{tc} \approx 1.0$ exists for *t*-**2**/H$^+$ where the PET is deactivated, indicating a diabatic mechanism for *t*-**2***/H$^+$ → *c*-**2***/H$^+$. Therefore, the observation that $\Phi_{fl} + 2\Phi_{tc} \ll 1.0$ for neutral *t*-**2** can be attributed to the quenching of *t*-**2*** by the PET ($\Phi_{PET} \approx 0.66$; Appendix S1 in the Supporting Information).

Scheme 4. General Mechanistic Scheme for Cis−Trans Photoisomerization of Stilbenes, Where *t*, *c*, and *p* Stand for the Trans, Cis, and Perpendicularly Twisted Isomers, Respectively

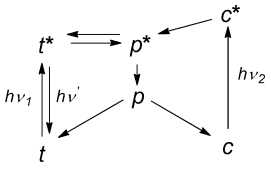

In spite of the PET, a surprisingly large Φ_{ct} (0.68) was observed for *c*-**2**, indicating a highly efficient adiabatic *c*-**2*** → *t*-**2*** photoisomerization (Scheme 4, where the *p** → *t** process is significant). On the basis of the known excited-state behavior of *t*-**2**/H$^+$ and the value of Φ_{ct} for *c*-**2**/H$^+$ (0.64), the relative efficiency of the adiabatic *c*-**2***/H$^+$ → *p*-**2***/H$^+$ → *t*-**2***/H$^+$ pathway was estimated to be ∼76%. The fact that the same value of 76% was obtained from the ratio Φ_{fl}(*c*-**2***/H$^+$)/Φ_{fl}(*t*-**2***/H$^+$) indicates that the adiabatic isomerization is via the singlet excited state (Appendix S1 in the Supporting Information). This is in sharp contrast to the famous anthrylethylene systems, which undergo triplet-state adiabatic cis → trans isomerization.[10] To the best of our knowledge, this has been the highest quantum efficiency for ssad cis → trans photoisomerization.[9,11] The same analysis for *c*-**2** indicates that ∼13% of the excited state is quenched by the PET before it forms *p*-**2*** (Appendix S1 in the Supporting Information).

Scheme 2b outlines the performance of the molecular ABS *t*-**2**. At 375 nm, the brake is turned on with the antilock function and forms the brake-on state *c*-**2** in >99% yield. A fast return of *c*-**2** back to the brake-off *t*-**2** state was performed by irradiation with 250 nm light. The recovery of *t*-**2** is 74%, leading to an overall switching power of ∼74%. To date, the number of stilbene- or azobenzene-derived light-gated molecular devices that possess a switching power higher than 70% is limited.[12,13] With the high braking power (∼10^7), the large ratio of Φ_{ct}/Φ_{tc} (5.2), and the fluorescence turn-on alarm, *t*-**2** proves the concept of a light-gated molecular ABS.

Figure 3 shows an experiment of five consecutive cycles of on−off switching of the brake monitored by the fraction of *t*-**2**.

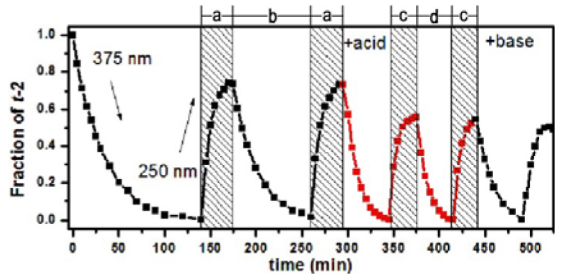

Figure 3. Plot of the fraction of *t*-**2** against the irradiation time for *t*-**2** at alternating wavelengths of 375 and 250 nm in acetonitrile. The black and red curves are at 0.0 and 10.0 equiv of $HClO_4$, respectively. KO^{t}Bu was the base for neutralization.

The first two cycles are in the neutral form, the third and fourth cycles are in the presence of $HClO_4$, and the last one is in the neutral form again after the addition of KO^{t}Bu. The ABS behavior, as evaluated by the relative times for the *t*-**2** → *c*-**2** and *c*-**2** → *t*-**2** conversions, is more obvious in the neutral form than the protonated form (b/a = 2.43 vs d/c = 1.33). In addition, the recovery of *t*-**2** decreased by ∼18% in the presence of $HClO_4$ and remained so even after neutralization, showing an undesired side effect of acid and base treatments. Therefore, removal of chemicals for the ABS operation is advantageous not only in the convenience of operation but also in enhancing the switching power.

In conclusion, the potential utility of π-extended stilbene chromophores that undergo efficient singlet-state adiabatic cis → trans isomerization for the design of high-performance light-gated molecular devices has been demonstrated with the molecular ABS *t*-**2**.

EXPERIMENTAL SECTION

General Methods. 1D ^{1}H (400 and 500 MHz) and ^{13}C (100 and 125 MHz) and 2D COSY, NOESY, and HSQC NMR spectra were acquired with 5 mm gradient triple-resonance broadband inverse (TBI) or triple-resonance broadband observe (TBO) probes. The chemical shifts for ^{1}H and ^{13}C spectra were referenced to the signals of tetramethylsilane [$\delta(^1H)$ = 0 ppm and $\delta(^{13}C)$ = 0 ppm]. Single-pulse spectra were recorded using a 308 pulse and a suitable delay time (2 and 6 s for ^{1}H and ^{13}C, respectively). For variable-temperature measurements, the actual sample temperature was well-calibrated by ^{1}H signals of ethylene glycol and methanol so that the temperature error was assured to be within ±1 K. Signal acquisition was begun after a sufficient temperature equilibration time (10−15 min). Fitting of dynamic NMR spectroscopic line shapes at different temperatures was performed with the Topspin 2.0 program.

UV−vis absorption and fluorescence spectra were measured at room temperature, and the latter were corrected for the response of the detector. The optical density (OD) of each solution was about 0.1 at the wavelength of excitation. Nitrogen-outgassed solutions of diphenylanthracene (Φ_f = 0.93 in cyclohexane)[14] and anthracene (Φ_f = 0.27 in hexane)[15] were used as standards for the fluorescence quantum yield determinations of compounds **2** and **4**, respectively, in

dx.doi.org/10.1021/jo5007015 | J. Org. Chem. 2014, 79, 6321−6325

N_2-outgassed solutions with solvent refractive index correction. An error of 10% is estimated for the fluorescence quantum yields.

Quantum yields of photoisomerization were measured for optically dense degassed solutions (1×10^{-3} M) irradiated at 313 nm using a 75 W Xe arc lamp and a monochromator. *trans*-4-(*N*-Phenylamino)-stilbene was used as a reference standard ($\Phi_{tc} = 0.34$ in CH_2Cl_2).[16] The extent of photoisomerization (<10%) was determined by HPLC analysis (3:7 hexane/ethyl acetate mixed solvent as the eluent and 1×10^{-3} M 1,4-dioctyloxybenzene as an internal standard) without back-reaction corrections. The reproducibility error was <10% of the average. The quantum yield for the trans → cis isomerization (Φ_{tc}) was determined using the following equation:

$$\frac{C_1 \times V_1 \times P_1}{\Phi_{tc1} \times t_1} = \frac{C_2 \times V_2 \times P_2}{\Phi_{tc2} \times t_2}$$

where C is the substrate concentration, V is the solution volume, P is the percentage of substrate that is converted to the cis isomer after irradiation, and t is the irradiation time. The subscripts 1 and 2 denote the reference standard and the substrate *t*-**2**, respectively. The same method was applied to the measurements of the cis → trans isomerization quantum yield (Φ_{ct}). In all cases, the HPLC traces showed the formation of a single product, corresponding to the cis or trans isomer.

Photoswitching experiments were conducted with stirring on 3 mL N_2-bubbled acetonitrile solutions (1.0×10^{-5} M) at selected wavelengths (375 nm for *t*-**2** → *c*-**2** and 250 nm for *c*-**2** → *t*-**2**) using a 75 W Xe arc lamp and a monochromator. The reactions were monitored by recording the UV absorption spectrum every minute for every 10 min of irradiation. The fraction of *t*-**2** in the mixture of *t*-**2** and *c*-**2** was calculated by linear interpolation of the molar absorptivity at 320 nm between the known values for *t*-**2** (36 000 M^{-1} cm^{-1}) and *c*-**2** (22 200 M^{-1} cm^{-1}) in acetonitrile. For the purpose of protonation of the amino group of *t*-**2** and *c*-**2**, to the solution was added 30 μL of 10^{-2} M $HClO_4$ in acetonitrile, prepared from 0.1 mL of concentrated $HClO_4$(aq) in 10 mL of acetonitrile. To neutralize the solution, 30 μL of 10^{-2} M KO^{t}Bu(aq) was added to the solution.

Materials. *Synthesis of t-2.* A mixture of **3** (2.2 g, 3.4 mmol), $Pd(OAc)_2$ (40 mg, 0.18 mmol), PPh_3 (80 mg, 0.26 mmol), **4** (0.75g, 3.7 mmol), DMF (15 mL), and triethylamine (3 mL) was heated to 90 °C for 16 h under argon. The mixture was concentrated under reduced pressure, and the residue was dissolved in EA and washed with brine. The organic layer was dried over anhydrous $MgSO_4$, and the filtrate was concentrated under reduced pressure. Preparative HPLC with *n*-hexane/CH_2Cl_2 (1:1 v/v) as the eluent afforded the product in 54% yield. Mp >300 °C; ^{1}H NMR (400 MHz, $CDCl_3$) δ = 2.54 (s, 6H), 3.01 (t, J = 6.0 Hz, 2H), 4.04 (t, J = 6.0 Hz, 2H), 5.72 (s, 2H), 5.76 (s, 2H), 6.76 (d, J = 16.4 Hz, 2H), 6.92–6.97 (m, 8H), 7.27–7.35 (m, 8H), 7.61 (d, J = 16.4 Hz, 2H), 7.76–7.84 (m, 8H) ppm; ^{13}C NMR (100 MHz, $CDCl_3$) δ = 46.3, 48.2, 51.2, 59.4, 73.6, 111.1, 123.5 (2C), 125.1, 125.2, 127.4, 127.6, 127.8 (2C), 132.8, 135.0, 135.4, 137.6, 138.7, 142.4, 145.1, 145.4, 149.1 ppm; IR (KBr) 2224 (CN) cm^{-1}; HRMS (FAB-ion trap) calcd for $C_{53}H_{40}N_2O$ m/z 720.3141 [M^+], found 720.3137.

Synthesis of c-2. A N_2-purged solution of *t*-**2** in dichloromethane (1 mm) was irradiated at 365 nm in a Rayonet photochemical reactor for 60 min. The solvent was removed under reduced pressure. Preparative HPLC with *n*-hexane/CH_2Cl_2 (1:1 v/v) as the eluent afforded the product in 83% yield. Mp >300 °C; ^{1}H NMR (500 MHz, CD_2Cl_2) δ = 2.54 (s, 6H), 3.00 (t, J = 6.4 Hz, 2H), 4.09 (t, J = 6.4 Hz, 2H), 5.44 (s, 2H), 5.72 (s, 2H), 6.54 (br, 4H), 6.80–7.00 (br, 11H), 7.05 (d, J = 8 Hz, 2H), 7.12 (d, J = 12 Hz, 1H), 7.26–7.30 (m, 4H), 7.44 (dd, J = 8.0 and 1.6 Hz, 2H), 7.63 (dd, J = 8.0 and 1.6 Hz, 2H) ppm; ^{13}C NMR (125 MHz, CD_2Cl_2) δ = 46.0, 48.4, 51.6, 111.1, 119.2, 123.5, 123.7, 123.9 (2C), 125.0 (2C), 125.3, 125.4, 125.5, 125.6, 126.6, 127.5, 127.7, 129.9, 132.9, 133.1, 133.4, 135.7, 137.4, 138.2, 142.4, 145.2, 145.3, 145.5, 145.7, 145.9 ppm; IR (KBr) 2225 (CN) cm^{-1}; HRMS (FAB-ion trap) calcd for $C_{53}H_{40}N_2O$ m/z 720.3141 [M^+], found 720.3149.

■ ASSOCIATED CONTENT

Supporting Information

1D, 2D, and VT NMR spectra, Arrhenius and Eyring plots, and VT excitation and fluorescence spectra. This material is available free of charge via the Internet at http://pubs.acs.org.

■ AUTHOR INFORMATION

Corresponding Author

*E-mail: jsyang@ntu.edu.tw.

Notes

The authors declare no competing financial interest.

■ ACKNOWLEDGMENTS

Financial support for this research was provided by the Ministry of Science and Technology and National Taiwan University (Excellence Research Project 103R891303).

■ REFERENCES

(1) (a) Kottas, G. S.; Clarke, L. I.; Horinek, D.; Michl, J. *Chem. Rev.* **2005**, *105*, 1281–1376. (b) Kinbara, K.; Aida, T. *Chem. Rev.* **2005**, *105*, 1377–1400. (c) Kay, E. R.; Leigh, D. A.; Zerbetto, F. *Angew. Chem., Int. Ed.* **2007**, *46*, 72–191. (d) Feringa, B. L. *J. Org. Chem.* **2007**, *72*, 6635–6652. (e) Coskun, A.; Banaszak, M.; Astumian, R. D.; Stoddart, J. F.; Grzybowski, B. A. *Chem. Soc. Rev.* **2012**, *41*, 19–30.

(2) (a) Kelly, T. R.; Bowyer, M. C.; Bhaskar, V.; Bebbington, D.; Garcia, A.; Lang, F.; Kim, M. H.; Jette, M. P. *J. Am. Chem. Soc.* **1994**, *116*, 3657–3658. (b) Nikitin, K.; Müller-Bunz, H.; Ortin, Y.; McGlinchey, M. J. *Chem.—Eur. J.* **2009**, *15*, 1836–1843. (c) Zhang, D.; Zhang, Q.; Sua, J. H.; Tian, H. *Chem. Commun.* **2009**, 1700–1702. (d) Chong, Y. S.; Dial, B. E.; Burns, W. G.; Shimizu, K. D. *Chem. Commun.* **2012**, *48*, 1296–1298.

(3) (a) Schoevaars, A. M.; Kruizinga, W.; Zijlstra, R. W. J.; Veldman, N.; Spek, A. L.; Feringa, B. L. *J. Org. Chem.* **1997**, *62*, 4943–4948. (b) ter Wiel, M. K. J.; van Delden, R. A.; Meetsma, A.; Feringa, B. L. *Org. Biomol. Chem.* **2005**, *3*, 4071–4076. (c) Basheer, M. C.; Oka, Y.; Mathews, M.; Tamaoki, N. *Chem.—Eur. J.* **2010**, *16*, 3489–3496.

(4) (a) Yang, J.-S.; Huang, Y.-T.; Ho, J.-H.; Sun, W.-T.; Huang, H.-H.; Lin, Y.-C.; Huang, S.-J.; Huang, S.-L.; Lu, H.-F.; Chao, I. *Org. Lett.* **2008**, *10*, 2279–2282. (b) Sun, W.-T.; Huang, Y.-T.; Huang, G.-J.; Lu, H.-F.; Chao, I.; Huang, S.-L.; Huang, S.-J.; Lin, Y.-C.; Ho, J.-H.; Yang, J.-S. *Chem.—Eur. J.* **2010**, *16*, 11594–11604.

(5) (a) Chen, Y.-C.; Sun, W.-T.; Lu, H.-F.; Chao, I.; Huang, G.-J.; Lin, Y.-C.; Huang, S.-L.; Huang, H.-H.; Lin, Y.-D.; Yang, J.-S. *Chem.—Eur. J.* **2011**, *17*, 1193–1200. (b) Yang, C.-H.; Prabhakar, C.; Huang, S.-L.; Lin, Y.-C.; Tan, W. S.; Misra, N. C.; Sun, W.-T.; Yang, J.-S. *Org. Lett.* **2011**, *13*, 5632–5635.

(6) Sun, W.-T.; Huang, S.-L.; Yao, H.-H.; Chen, I. C.; Lin, Y.-C.; Yang, J.-S. *Org. Lett.* **2012**, *14*, 4154–4157.

(7) (a) Mollenhauer, M. A.; Dingus, T. A.; Carney, C.; Hankey, J. M.; Jahns, S. *Accid. Anal. Prev.* **1997**, *29*, 97–108. (b) Forkenbrock, G.; Flick, M.; Garrott, W. R. *A Comprehensive Light Vehicle Antilock Brake System Test Track Performance Evaluation*; SAE Technical Paper 1999-01-1287; Society of Automotive Engineers: Warrendale, PA, 1999.

(8) Ballav, N.; Schüpbach, B.; Dethloff, O.; Feulner, P.; Terfort, A.; Zharnikov, M. *J. Am. Chem. Soc.* **2007**, *129*, 15416–15417.

(9) (a) Sandros, K.; Sundahl, M.; Wennerström, O.; Norinder, U. *J. Am. Chem. Soc.* **1990**, *112*, 3082–3086. (b) Bartocci, G.; Galiazzo, G.; Marri, E.; Mazzucato, U.; Spalletti, A. *Inorg. Chim. Acta* **2007**, *360*, 961–969. (c) Bartocci, G.; Ciorba, S.; Mazzucato, U.; Spalletti, A. *J. Phys. Chem. A* **2009**, *113*, 8557–8568. (d) Saltiel, J.; Kumar, V. K. R.; Reedwood, C. E.; Mallory, F. B.; Mallory, C. W. *Photochem. Photobiol. Sci.* **2014**, *13*, 172–181.

(10) For triplet-state adiabatic photoisomerization, see: Arai, T.; Tokumaru, K. *Chem. Rev.* **1993**, *93*, 23–39.

(11) Saltiel, J.; Waller, A. S.; Sears, D. F., Jr. *J. Am. Chem. Soc.* **1993**, *115*, 2453–2465.

(12) (a) Koumura, N.; Zijlstra, R. W. J.; van Delden, R. A.; Harada, N.; Feringa, B. L. *Nature* **1999**, *401*, 152−155. (b) Koumura, N.; Geertsema, E. M.; Meetsma, A.; Feringa, B. L. *J. Am. Chem. Soc.* **2000**, *122*, 12005−12006.
(13) (a) Muraoka, T.; Kinbara, K.; Aida, T. *Chem. Commun.* **2007**, 1441−1443. (b) Coskun, A.; Friedman, D. C.; Li, H.; Patel, K.; Khatib, H. A.; Stoddart, J. F. *J. Am. Chem. Soc.* **2009**, *131*, 2493−2495.
(14) Birks, J. B. *Photophysics of Aromatic Molecules*; Wiley-Interscience: London, 1970.
(15) Dawson, W. R.; Windsor, M. W. *J. Phys. Chem.* **1968**, *72*, 3251−3260.
(16) Yang, J.-S.; Liau, K.-L.; Wang, C.-M.; Hwang, C.-Y. *J. Am. Chem. Soc.* **2004**, *126*, 12325−12335.

dx.doi.org/10.1021/jo5007015 | *J. Org. Chem.* 2014, 79, 6321−6325